Aalborg Universitet

A Reduced-Order Enhanced State Observer Control of DC-DC Buck Converter

JINGHANG LU[1], (Student Member, IEEE), MEHDI SAVAGHEBI[2], (Senior Member, IEEE), YAJUAN GUAN[1], (Member, IEEE), JUAN C. VASQUEZ[1], (Senior Member, IEEE), AMER M. Y. M. GHIAS[3], (Member, IEEE), AND JOSEP M. GUERRERO[1], (Fellow, IEEE)

[1]Department of Energy Technology, Aalborg University, DK-9220 Aalborg, Denmark
[2]Department of Electrical Engineering, University of Southern Denmark, DK-5230 Odense, Denmark
[3]Department of Electrical and Electronic Engineering, Nanyang Technological University, Singapore 639798

Corresponding author: Yajuan Guan (ygu@et.aau.dk)

ABSTRACT This paper presents a reduced-order-enhanced state observer (RESO)-based control strategy for the PWM dc–dc buck converter. With the proposed RESO control strategy, the output voltage regulation of the dc–dc buck converter is able to achieve robust characteristics against the external disturbance and the internal parameter variation even without output current measurement. In addition, by incorporating the RESO in the controller, the output voltage regulation can be easily achieved with only a proportional gain to realize a zero steady-state error. Finally, the parameter design is discussed and the effectiveness of the proposed control strategy is verified with an experimental case study.

INDEX TERMS DC-DC buck converter, disturbance rejection, reduced-order enhanced state observer, robustness, system parameter variation.

I. INTRODUCTION

In the last few decades, the DC-DC buck converters have been commonly applied in the industrial systems, such as DC motor drive, more electrical aircraft, electric vehicles, dc microgrid, etc [1]–[4]. In such applications, the DC-DC buck converter needs to precisely regulate its output voltage. It is, however, still a challenging task, as various factors, such as: load sudden change and system parameter variation, may greatly affect the precise regulation of the output voltage [5]. Thus, to obtain a satisfactory performance, it is required for the controller to achieve a high disturbance rejection capability, a zero steady-state error, a small overshoot and a fast dynamic response during the transient process [6].

Because of its simplicity, a proportional-integral (PI) or proportional-integral-differential (PID) control strategy is usually adopted to regulate the DC-DC buck converter, but it always leads to the poor performance if large disturbance and system uncertainties exist in the system [7]. In order to alleviate the disturbance influence on the voltage regulation, a feedforward controller is usually added in the control system [8], [9]. However, the feedforward control strategy cannot detect/compensate the system parameter variation. To conquer this issue, several advanced control methods have been recently presented and adopted for the DC-DC buck converter [1], [2], [10]–[14]. Among these

studies, [5] and [12] have proposed the sliding mode-based control strategy for the DC-DC converter. However, the disturbance rejection ability of these methods still needs to be improved. In order to deal with the aforementioned issue, [14] and [15] proposed an observer-based sliding mode control strategy to overcome the matched and mismatched disturbances of the buck converter, which showed good performance in disturbance rejection. However, as the nonlinear control strategies are implemented, it is quite difficult to analyze the system's performance and design the controller. Besides, the chattering issue in the sliding mode control may cause high-frequency harmonics, which demands special attention. Other control methods, such as robust control [13], adaptive control [16], geometric control [17], may also be adopted to the DC-DC converter. The nonlinear nature of these approaches, however, makes their implementation difficult for a practical engineer. In addition, all the aforementioned works adopt a single-loop control strategy for the output voltage regulation. However, compared to a dual-loop control strategy, which simultaneously regulates the inductor current and the capacitor voltage of the DC-DC converter, the single-loop one may not be able to directly regulate the inductor's current from overshoot during the transients [7]. Without such regulation, system may be tripped due to the current overshoot particularly when the load is suddenly

connected or disconnected. In [10], a reduced-order generalized proportional integral (GPI) observer-based model predictive control strategy is suggested for the DC-DC buck converter. This method offers good performance in rejecting the disturbance, but selecting its control parameters is quite difficult. Notice that these parameters are inside a cost function, and, therefore, it is quite complicated to establish a connection between them and the control performance indices, such as settling time, overshoot, and the damping ratio of the system.

Recently, the enhanced state observer, which is proposed by [18], has been successfully implemented for the DC-link voltage control. Inspired by [18], a reduced-order enhanced state observer (RESO)-based proportional controller is proposed for the output voltage regulation of a DC-DC buck converter. With the proposed control strategy, system's fast disturbance rejection ability and the strong robustness against the parameter variation are achieved. In addition, the frequency domain analysis of the RESO is first presented to provide an insight into RESO's compensation for the disturbance and present a guideline on designing the RESO. The design principle is based on the state observer's bandwidth ω_0, which can be easily implemented by the engineers. Finally, the proposed method is verified with experimental results.

II. MODELING OF THE DC-DC BUCK CONVERTER
A. DYNAMIC MODELING OF THE DC-DC BUCK CONVERTER

As shown in Fig.1, the circuit diagram of the DC-DC buck converter is comprised of a PWM MOSFET SW, a DC voltage source V_{in}, a diode, an inductor L with its associated parasitic resistance r_L, a capacitor, a parallel resistor r_c and the load (which is here assumed to be a resistor R). It is noted that the parallel resistor r_c acts to discharge the capacitor as a protection method [19]. In addition, r_c can be considered as the system parameter variation, and this system parameter variation will be considered as an additional state variable that is estimated and cancelled by RESO as explained in the next section. Hence, the dynamic average model of the buck converter is expressed as:

$$\begin{cases} \dfrac{dv_o(t)}{dt} = \dfrac{1}{C}i_L(t) - \dfrac{1}{C}i_o(t) - \dfrac{1}{C}\dfrac{v_o(t)}{r_C} & (1a) \\ \dfrac{di_L(t)}{dt} = \dfrac{1}{L}m(t)\,V_{in}(t) - \dfrac{1}{L}r_L i_L(t) - \dfrac{1}{L}v_o(t) & (1b) \end{cases}$$
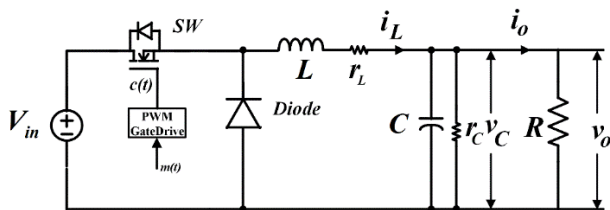

FIGURE 1. Circuit diagram of a DC-DC buck converter.

where v_o is the average output capacitor voltage, $i_L(t)$ is the average inductor current, and $m(t)$ is the PWM input signal respectively.

The Laplace transform of the Eq.(1a) results in:

$$v_o(s) = \frac{r_C}{Cr_C s + 1}i_L(s) - \frac{r_C}{Cr_C s + 1}i_o(s) \qquad (2)$$

As mentioned before, a cascaded dual-loop control approach is often recommended for the control of the DC-DC buck converter instead of using a single-loop output voltage regulation. In the dual-loop control, a wide bandwidth current regulation loop is nested inside a narrow bandwidth voltage control loop. The main benefit of this control approach is the direct regulation/limitation of the converter current, which gives an overcurrent protection feature to it. Meanwhile, the dual-loop strategy ensures that the current sharing in a system with multiple DC-DC buck converters (a DC microgrid application) is satisfactorily performed [1].
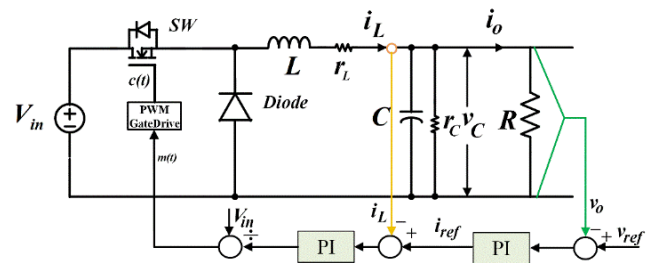

FIGURE 2. Power stage of the DC-DC Buck converter with traditional PI -based cascaded dual-loop control strategy.

A typical dual-loop control strategy with the power stage of the DC-DC converter is shown in Fig. 2, where the dual PI controllers are adopted to regulate the output voltage and inductor current. In order to improve the dynamic performance under the disturbances, the feedforward control strategy by measuring the output current should be added to the control structure. It, however, requires an additional sensor, which inevitably increases the cost and reduces the reliability of the system. In addition, any uncertainty in the system, particularly parameters variations, cannot be directly measured by the feedforward control strategy. Therefore, in what follows, a RESO-based observer is designed to achieve an enhanced dynamic system performance under disturbances and system uncertainties.

B. REDUCED-ORDER ENHANCED STATE OBSERVER DESIGN

The proposed complete control diagram of the buck converter is shown in Fig.3. The control structure consists of the RESO-based output voltage loop and an inner current loop to regulate the inductor's current. The detailed control structure of the proposed dual-loop control strategy is shown in Fig.4 for the DC-DC buck converter. Normally, in order to design the dual loops, the dynamic of the outer voltage loop is considered to be much slower than that of the inner current loop. It indicates that dynamics of the inductor's
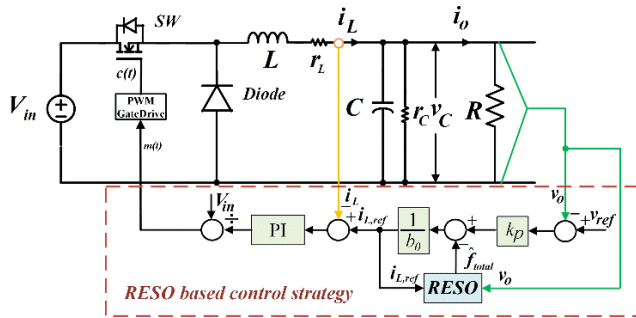
FIGURE 3. Diagram of the DC-DC buck converter with the RESO-based control strategy.

current closed-loop transfer function can be considered as a one when designing the outer voltage loop, in other words, it is assumed that $i_L \cong i_{L\_ref}$, where i_L and i_{L_ref} are the inductor's actual and reference currents, respectively (Fig. 4). This approximation decouples the dynamics of these two loops and greatly simplifies the controller's design.

As shown in Fig.4, the proposed output voltage control strategy is comprises of a RESO and a proportional controller. The RESO is adopted to estimate and cancel the system disturbances/uncertainties in real time; then, only a proportional controller is able to regulate the output voltage without steady-state error. In the following section, the RESO is first constructed and the design procedure is discussed. Then, the proportional controller is discussed.

Equation (1a) can be expressed as:

$$\frac{dv_o(t)}{dt} = \frac{1}{C}i_L(t) - \frac{1}{C}i_o(t) - \frac{1}{C}\frac{v_o}{r_C} = \frac{1}{C}i_L(t) + f_{total} \tag{3}$$

where f_{total} indicates the total disturbance that include external disturbance $(-\frac{1}{C}i_o(t))$, system parameter variation $((-\frac{1}{C}\frac{v_o}{r_C}))$ and other unmodeled disturbance, such as electromagnetic interference (EMI) of the capacitance.

By considering that v_o, f_{total} and $\dot{f}_{total}$ are the system state variables, the corresponding state-space model can be written as:

$$\begin{bmatrix} \dot{x}_1 \\ \dot{x}_2 \\ \dot{x}_3 \end{bmatrix} = \begin{bmatrix} 0 & 1 & 0 \\ 0 & 0 & 1 \\ 0 & 0 & 0 \end{bmatrix}\begin{bmatrix} x_1 \\ x_2 \\ x_3 \end{bmatrix} + \begin{bmatrix} b_0 \\ 0 \\ 0 \end{bmatrix}u + \begin{bmatrix} 0 \\ 0 \\ 1 \end{bmatrix}h \tag{4}$$

where $x_1 = v_o$, $x_2 = f_{total} = -\frac{1}{C}i_o(t) - \frac{1}{C}\frac{v_o}{r_C}$, $x_3 = \dot{f}_{total}$, $u = i_{Lref}$ $b_0 = \frac{1}{C}$, $h = \frac{dx_3}{dt}$.

Hence, the high-order ESO (HESO) is constructed as:

$$\begin{bmatrix} \dot{\xi}_1 \\ \dot{\xi}_2 \\ \dot{\xi}_3 \end{bmatrix} = \begin{bmatrix} 0 & 1 & 0 \\ 0 & 0 & 1 \\ 0 & 0 & 0 \end{bmatrix}\begin{bmatrix} \xi_1 \\ \xi_2 \\ \xi_3 \end{bmatrix} + \begin{bmatrix} b_0 \\ 0 \\ 0 \end{bmatrix}u + \begin{bmatrix} b_1 \\ b_2 \\ b_3 \end{bmatrix}[x_1 - \xi_1] \tag{5}$$

where ξ_1, ξ_2, and ξ_3 are the estimations of x_1, x_2, x_3, $\begin{bmatrix} b_1 \\ b_2 \\ b_3 \end{bmatrix}$ is the observer's gain.

In order to increase the HESO's estimation ability and also reduce the computation burden due to the high-order estimation, a new RESO, instead of the high-order ESO, is proposed for the voltage control of the DC-DC buck converter, as explained below.

By re-writing Eq.(4), the following equation is derived:

$$\begin{bmatrix} \dot{x}_2 \\ \dot{x}_3 \end{bmatrix} = \begin{bmatrix} 0 & 1 \\ 0 & 0 \end{bmatrix}\begin{bmatrix} x_2 \\ x_3 \end{bmatrix} + \begin{bmatrix} 0 \\ 1 \end{bmatrix}h \tag{6}$$

$$\dot{x}_1 - b_0 u = x_2 \tag{7}$$

Therefore, the RESO is designed as:

$$\begin{bmatrix} \dot{\xi}_2 \\ \dot{\xi}_3 \end{bmatrix} = \begin{bmatrix} 0 & 1 \\ 0 & 0 \end{bmatrix}\begin{bmatrix} \xi_2 \\ \xi_3 \end{bmatrix} - \begin{bmatrix} k_1 & 0 \\ k_2 & 0 \end{bmatrix}\begin{bmatrix} \xi_2 \\ \xi_3 \end{bmatrix} + \begin{bmatrix} k_1\dot{x}_1 \\ k_2\dot{x}_1 \end{bmatrix} - \begin{bmatrix} k_1 b_0 u \\ k_2 b_0 u \end{bmatrix} \tag{8}$$

where $\begin{bmatrix} k_1 \\ k_2 \end{bmatrix}$ is the RESO gain, ξ_2 and ξ_3 are the estimated value of x_2 and x_3.

However, in (8), the variable $\dot{x}_1$ cannot be directly measured, hence, by manipulating $\begin{bmatrix} k_1\dot{x}_1 \\ k_2\dot{x}_1 \end{bmatrix}$ into the left hand of the equation, meanwhile, by adding and substracting the term $\begin{bmatrix} -k_1 & 1 \\ -k_2 & 0 \end{bmatrix}\begin{bmatrix} k_1 x_1 \\ k_2 x_2 \end{bmatrix}$, the following equations are derived as:

$$\begin{bmatrix} \dot{\xi}_2 \\ \dot{\xi}_3 \end{bmatrix} - \begin{bmatrix} k_1\dot{x}_1 \\ k_2\dot{x}_1 \end{bmatrix} = \begin{bmatrix} -k_1 & 1 \\ -k_2 & 0 \end{bmatrix}\left\{\begin{bmatrix} \xi_2 \\ \xi_3 \end{bmatrix} - \begin{bmatrix} k_1 x_1 \\ k_2 x_1 \end{bmatrix}\right\}$$
$$- \begin{bmatrix} k_1 b_0 u \\ k_2 b_0 u \end{bmatrix} + \begin{bmatrix} -k_1 & 1 \\ -k_2 & 0 \end{bmatrix}\begin{bmatrix} k_1 x_1 \\ k_2 x_1 \end{bmatrix} \tag{9}$$

Based on (5) and (9) that signals f_{total} and $\dot{f}_{total}$ both can be observed by the HESO and the RESO. However, the order of the presented RESO is only two. This reduced order observer can alleviate the computation burden compared with the full order one. In addition, it will be shown in subsection. F that with the RESO, the controller's design will be greatly simplified.

C. SYSTEM STABILITY ANALYSIS

The system stability can be analyzed by subtracting Eq.(6) from Eq.(8), the error of these two equations is written as:

$$\begin{bmatrix} \dot{e}_2 \\ \dot{e}_3 \end{bmatrix} = \underbrace{\begin{bmatrix} -k_1 & 1 \\ -k_2 & 0 \end{bmatrix}}_{N_e}\begin{bmatrix} e_2 \\ e_3 \end{bmatrix} + \begin{bmatrix} k_1\dot{x}_1 \\ k_2\dot{x}_1 \end{bmatrix} - \begin{bmatrix} b_0 u \\ b_0 u \end{bmatrix} \tag{10}$$

where e_2 is the difference between x_2 and ξ_2, and e_3 is the difference between x_3 and ξ_3 respectively. From (10), it can be found that if all of the roots of the matrix N_e are selected to be at the left half plane, the system will be stable.

Therefore, the desired roots of the polynomial of N_e are expressed as:

$$\mu(s) = s^2 + k_1 s + k_2 \tag{11}$$

In order to make the design process easy to be implemented, suppose the observer poles are both located at $-\omega_0$ and expressed as:

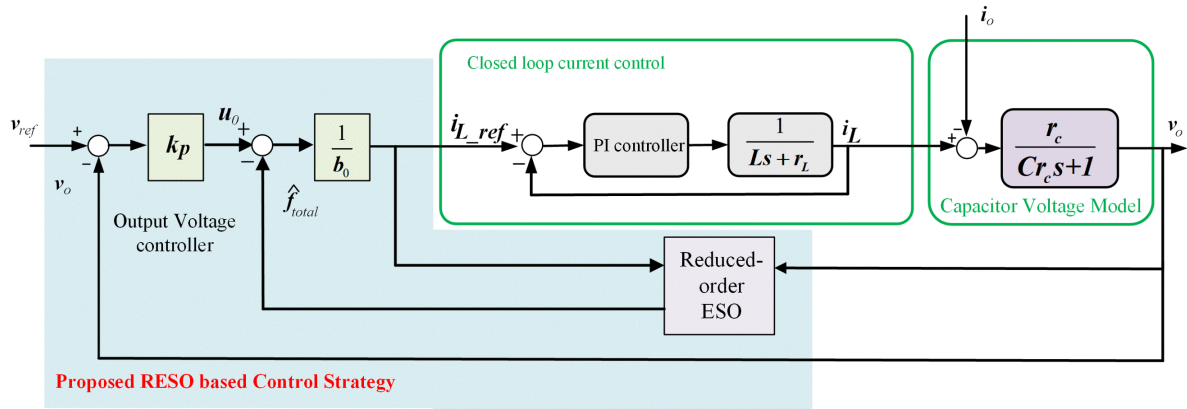$$\mu(s) = s^2 + k_1 s + k_2 = (s + \omega_0)^2 \tag{12}$$

FIGURE 4. Proposed structure diagram of output voltage control strategy with RESO.

Hence, $k_1 = 2\omega_0$, $k_2 = \omega_0^2$, In addition, it is found that the parameter selection of ω_0 is an important process that will influence the estimation accuracy and system dynamic response. Normally, the bandwidth of the RESO is specified to be much larger than the voltage controller's bandwidth, which indicates that the observer's bandwidth should be 10 times larger than the voltage controller's bandwidth. Meanwhile, observer's bandwidth should not be too large, as too large observer's bandwidth may inevitably reduce the system noise immunity. Therefore, the design procedure involves a tradeoff between accuracy and noise immunity. In this paper, in order to realize fast tracking ability, the inductor current controller's bandwidth is specified as 2000 rad/s. In addition, the RESO's bandwidth should not be selected to be over 1/3 of the current controller's bandwidth in order to decouple these two loops. Therefore, the RESO's bandwidth is designated for 600 rad/s. Finally, the voltage control loop possesses the slow dynamics and it needs to be decoupled from the RESO's bandwidth as well. So, the bandwidth of the voltage controller is set as 20 rad/s.

D. EQUIVALENT TRANSFER FUNCTION ANALYSIS IN FREQUENCY DOMAIN

By substituting $\xi_2 - k_1 x_1 = \zeta_2$ and $\xi_3 - k_2 x_1 = \zeta_3$. (9) is expressed as:

$$\begin{bmatrix} \dot{\zeta_2} \\ \dot{\zeta_3} \end{bmatrix} = \begin{bmatrix} -k_1 & 1 \\ -k_2 & 0 \end{bmatrix} \begin{bmatrix} \zeta_2 \\ \zeta_3 \end{bmatrix} + \begin{bmatrix} -k_1 b_0 & -k_1^2 + k_2 \\ -k_2 b_0 & -k_1 k_2 \end{bmatrix} \begin{bmatrix} u \\ x_1 \end{bmatrix} \tag{13}$$

By substituting $k_1 = 2\omega_0$, $k_2 = \omega_0^2$ into (13), the RESO is constructed as:

$$\begin{bmatrix} \dot{\zeta_2} \\ \dot{\zeta_3} \end{bmatrix} = \underbrace{\begin{bmatrix} -2\omega_0 & 1 \\ -\omega_0^2 & 0 \end{bmatrix}}_{A_z} \begin{bmatrix} \zeta_2 \\ \zeta_3 \end{bmatrix} + \begin{bmatrix} -2\omega_0 b_0 & -3\omega_0^2 \\ -\omega_0^2 b_0 & -2\omega_0^3 \end{bmatrix} \begin{bmatrix} u \\ x_1 \end{bmatrix} \tag{14}$$

(14) can be transformed into the transfer function by facilitating the following equation:

$$G_{\zeta_2\_u}(s) = \frac{\zeta_2(s)}{u(s)} = \begin{bmatrix} 1 & 0 \end{bmatrix} [sI - A_z]^{-1} \begin{bmatrix} -2\omega_0 b_0 \\ -\omega_0^2 b_0 \end{bmatrix}$$

$$= -\frac{b_0\omega_0^2}{(s+\omega_0)^2} - \frac{2b_0\omega_0 s}{(s+\omega_0)^2} \tag{15}$$

$$G_{\zeta_2\_v_o}(s) = \frac{\zeta_2(s)}{v_o(s)} = \begin{bmatrix} 1 & 0 \end{bmatrix} [sI - A_z]^{-1} \begin{bmatrix} -3\omega_0^2 \\ -2\omega_0^3 \end{bmatrix}$$

$$= -\frac{2\omega_0^3}{(s+\omega_0)^2} - \frac{3\omega_0^2 s}{(s+\omega_0)^2} \tag{16}$$

where $\xi_2 - k_1 x_1 = \zeta_2$, and $x_1 = v_o$, $k_1 = 2\omega_0$. Therefore, by combing (15) and (16) and substituting $z_2 - k_1 x_1 = \xi_2$, the transfer function of RESO is shown in Fig.5 and expressed as:

$$\hat{f}_{total}(s) = \left[-\frac{b_0\omega_0^2}{(s+\omega_0)^2} - \frac{2b_0\omega_0 s}{(s+\omega_0)^2} \right] u(s)$$

$$+ \frac{s\omega_0^2 + 2s^2\omega_0}{(s+\omega_0)^2} v_o(s) \tag{17}$$
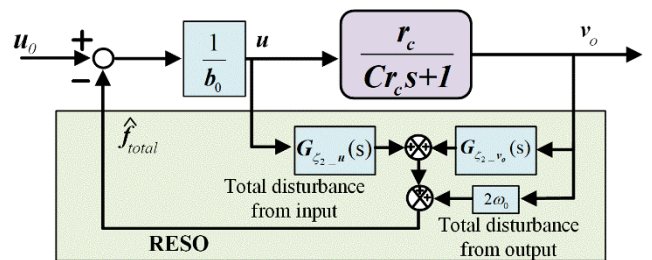
FIGURE 5. Frequency domain expression of RESO.

The modified model from $u_0(s)$ to $v_o(s)$ is written as the transfer function $\bar{G}_L(s)$:

$$\bar{G}_L(s) = \frac{v_o(s)}{u_o(s)} = \frac{\frac{G_L}{b_0}}{1 + \frac{G_{f\_u}}{b_0} + \frac{G_L G_{f\_vo}}{b_0}}$$

$$= \frac{G_L/b_0}{1 - \frac{1}{\left(\frac{s}{\omega_0}+1\right)^2} - \frac{2\left(\frac{s}{\omega_0}\right)}{\left(\frac{s}{\omega_0}+1\right)^2} + (\frac{G_L}{b_0})\frac{(s+\frac{2s}{2})}{\left(\frac{s}{\omega_0}+1\right)^2}} \tag{18}$$

where $G_L = \frac{r_C}{C r_C s + 1}$. Moreover, it can be easily derived from (18) that when the system's bandwidth is much less

than the RESO's bandwidth ($\omega \ll \omega_0$), the complicated transfer function of (18) is reduced to a pure integrator and written as:

$$\overline{G_L} \approx \frac{1}{s} \quad \omega \ll \omega_0 \tag{19}$$

On the contrary, when the system's bandwidth is much higher than the RESO's bandwidth, it will follow the original plant and expressed as:

$$\overline{G_L} \approx G_L/b_0 \quad \omega \gg \omega_0 \tag{20}$$

E. ROBUSTNESS EVALUATION AGAINST PARAMETER VARIATION

The output capacitance variation may affect the control performance and system stability. Hence, the closed-loop poles need to be investigated to ensure the controller's robustness against this uncertainty. In the system, the nominal value of the capacitance is 0.0022 F, but the output capacitance may vary from its nominal value, therefore, the evaluation of the pole's movement with the model $\overline{G_L}$ is conducted when the actual capacitance varies its value from 2200 uF to 5500 uF. It is observed in Fig.6 that when the output capacitance increases its value, the poles tend to move to the imaginary axis, which makes the system more oscillatory. But even when the capacitance reaches 0.0055 F, the system still provides a satisfactory robustness, as the poles' location are around -250rad/s, which are quite far away from the imaginary axis.
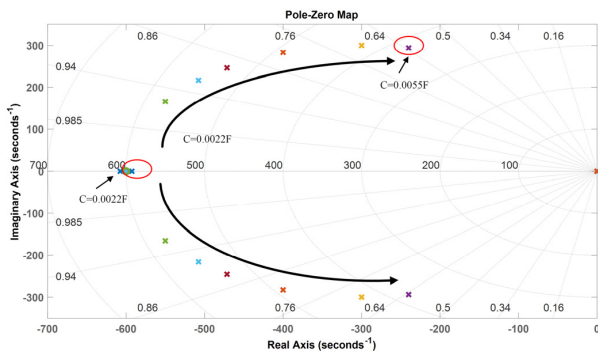

FIGURE 6. Pole's movement when system capacitor's parameter varies from 0.0022F to 0.055F

F. PROPORTIONAL GAIN CONTROL STRATEGY DERIVATION

From the previous discussion in section II.D, it was shown that within the bandwidth of RESO, the modified plant can be well-approximated by an integrator ($\overline{G_p} \approx \frac{1}{s}$). Considering this fact and the internal model principle, a simple proportional controller can realize the output voltage regulation with zero steady-state error. Moreover, the bandwidth of the output voltage controller can be decided by k_p. Hence, the closed-loop output voltage transfer function is expressed as:

$$G_{v_c} = \frac{k_p \frac{1}{s}}{1 + k_p \frac{1}{s}} = \frac{k_p}{k_p + s} = \frac{1}{1 + s/k_p} \tag{21}$$

In this paper, the bandwidth of the voltage loop is designated for 20 rad/s; therefore, $k_p = 20$.

III. EXPERIMENTAL RESULTS

In order to verify the effectiveness of the proposed control strategy, a DC-DC buck converter illustrated in Fig.1 is built up in Fig.7. Parameters of the power stage and controller are shown in Table 1. The dSPACE 1006 platform is used for controlling the DC-DC converter, and the figures are captured by an oscilloscope. In the experimental study, the sampling frequency f_s is chosen to be 10 kHz. Moreover, the PI control strategy for the voltage loop control and PI with feedforward control strategy for the voltage loop control of the DC-DC buck converter are evaluated and compared with the proposed control strategy. In order to have a fair comparison, these three control strategies have the same voltage loop and current loop bandwidth.
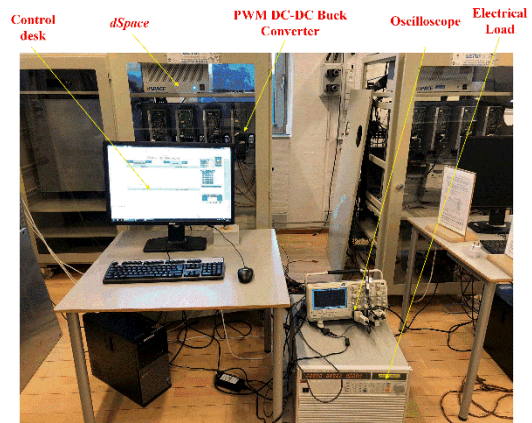

FIGURE 7. The experimental setup.

Test 1: In this test, the capacitor is selected to be 0.0022 F, A 25 ohm resistor is suddenly disconnected from the converter output and its performance in response to this sudden change is investigated. It can be observed in Fig.8 that PI controller performs an overshoot voltage that is equal to 16V and the settling time is around 0.2s, which shows the worst performance. Meanwhile, the feedforward-based PI controller has the overshoot voltage of 4V with the settling time of 0.2s as well. When the RESO-based control strategy is applied in the system, the overshoot in the system is similar with the one with the feedforward-based PI control strategy, but the recovery time reduced to 0.15s.

Test 2: In this test, system's capacitance parameter varies from 0.0022F to 0.0044F. System's dynamic performance under 100% increase of capacitance will be examined. The controller's parameters does not change in this test. The experimental results for this test are illustrated in Fig.9.

PI control strategy   PI with Feedforward   Proposed control strategy
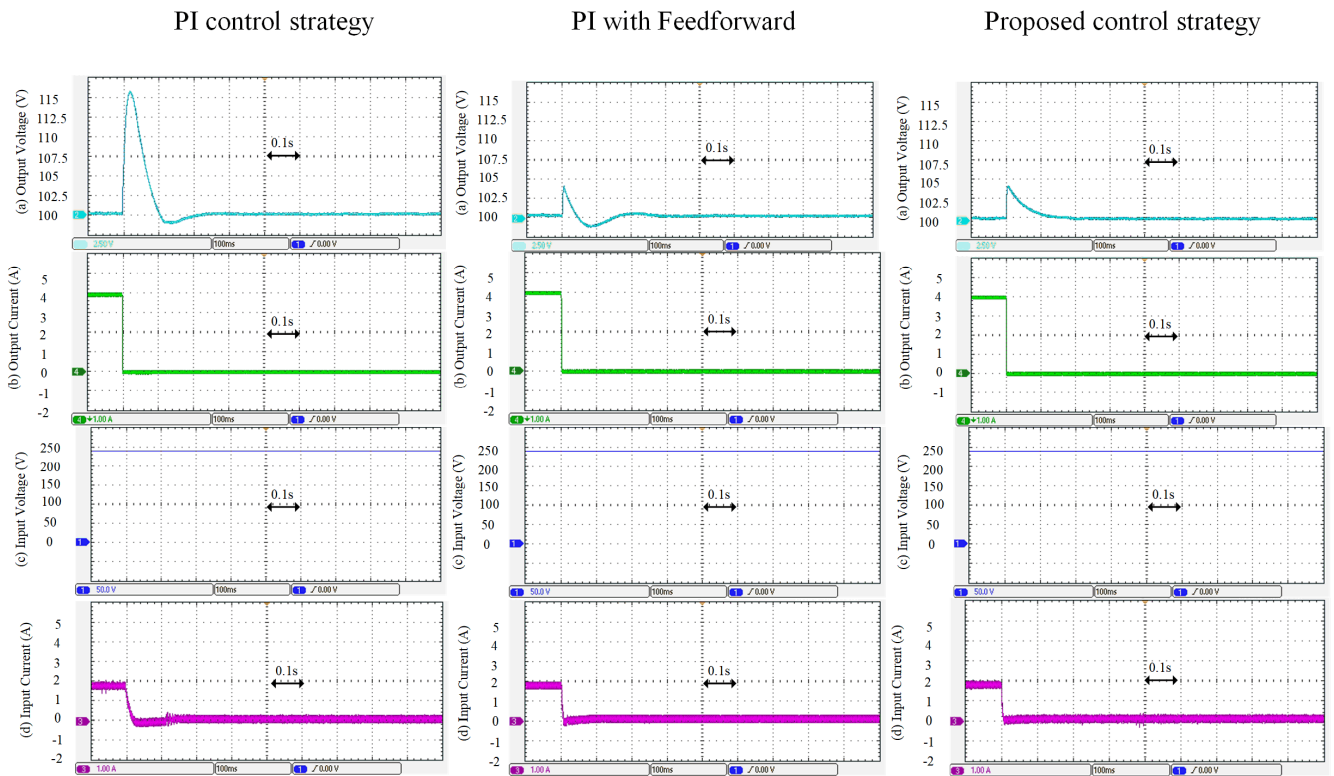
FIGURE 8. Performance comparison of the three control strategies under load disturbance when the output capacitor is 0.0022 F.

PI control strategy   PI with Feedforward   Proposed control strategy
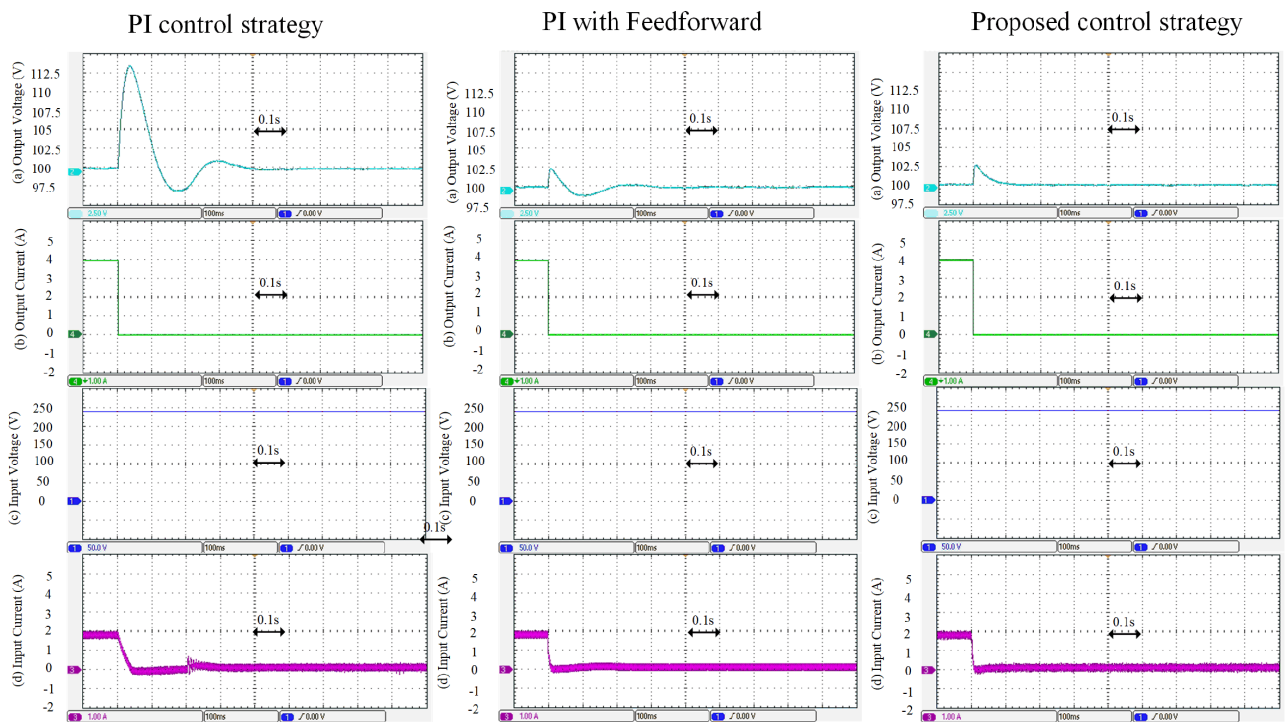
FIGURE 9. Performance comparison of the three control strategies under load disturbance when the output capacitor is 0.0044F.

As can be seen from Fig.9, when the traditional PI controller is applied, the voltage overshoot is reduced with more oscillation, and the settling time increased to 0.35s.

When the feedforward-based PI controller is applied, the voltage overshoot reduced to 2.5V, at the same time, the recovery time is 0.2s. Meanwhile, when the RESO-based control

TABLE 1. System parameters.

DC-DC Converter Parameters	
Filter inductor L	$1.8mH$
Inductor's parasitic resistance	0.02Ω
Normal capacitor C	$0.0022F$
Capacitor's parasitic resistance	1000Ω
Sampling frequency f_s	$10kHz$
DC load	25Ω
Input voltage	$240V$
Output voltage	$100V$
Control Parameters	
RESO bandwidth ω_0	600 rad/s
Proportional gain in voltage control strategy k_p	20
Proportional gain in current control strategy k_{pi}	7
Integral gain in current control strategy k_{pr}	200
PI Controller Parameters for comparison	
Proportional gain in voltage control	0.02
Integral gain in voltage control	0.1

strategy is adopted as the control strategy, the performance is the same as the feedforward-based PI control strategy with an overshoot of 2.5V and the settling time is reduced to 0.1s.

IV. CONCLUSION

In this paper, a RESO-based voltage control strategy was proposed for the voltage loop of the DC-DC buck converter. In addition, the proposed control strategy can achieve almost the same effect as feedforward control in disturbance rejection without needing the additional sensor as well as better ability in reducing the voltage overshoot and fasten the settling time. Moreover, the system's robustness against the parameter variation is discussed by checking the system's poles. Finally, the proposed control strategy is verified using experimental tests.

REFERENCES

[1] H. Wang, M. Han, R. Han, J. Guerrero, and J. C. Vasquez, "A decentralized current-sharing controller endows fast transient response to parallel DC–DC converters," *IEEE Trans. Power Electron.*, vol. 33, no. 5, pp. 4362–4372, May 2017.

[2] J. Sha, J. Xu, S. Zhong, S. Liu, and L. Xu, "Control pulse combination-based analysis of pulse train controlled DCM switching DC–DC converters," *IEEE Trans. Ind. Electron.*, vol. 62, no. 1, pp. 246–255, Jan. 2015.

[3] D. F. Cortez, G. Waltrich, J. Fraigneaud, H. Miranda, and I. Barbi, "DC–DC converter for dual-voltage automotive systems based on bidirectional hybrid switched-capacitor architectures," *IEEE Trans. Ind. Electron.*, vol. 62, no. 5, pp. 3296–3304, May 2015.

[4] J.-Y. Lee and H.-J. Chae, "6.6-kW onboard charger design using DCM PFC converter with harmonic modulation technique and two-stage DC/DC converter," *IEEE Trans. Ind. Electron.*, vol. 61, no. 3, pp. 1243–1252, Mar. 2014.

[5] S.-C. Tan, Y. M. Lai, and C. K. Tse, "General design issues of sliding-mode controllers in DC–DC converters," *IEEE Trans. Ind. Electron.*, vol. 55, no. 3, pp. 1160–1174, Mar. 2008.

[6] G. F. Franklin, J. D. Powell, and M. L. Workman, *Digital Control of Dynamic System*. Reading, MA, USA: Addison-Wesley, 1998.

[7] L. Corradini, D. Maksimovic, P. Mattavelli, and R. Zane, *Digital Control of High-Frequency Switched-Mode Power Converters*. Hoboken, NJ, USA: Wiley, 2015.

[8] G. F. Franklin, J. Powell, and A. Emami-Naeini, *Feedback Control of Dynamic Systems*, Global Ed. Pearson Education, 2015.

[9] W. Hu, E. F. Camacho, and L. Xie, "Feedforward and feedback control of dynamic systems," *IFAC Proc. Vol.*, vol., 47, no. 3, pp. 7741–7748, 2014.

[10] J. Yang, H. Cui, S. Li, and A. Zolotas, "Optimized active disturbance rejection control for DC-DC buck converters with uncertainties using a reduced-order GPI observer," *IEEE Trans. Circuits Syst. I, Reg. Papers*, vol. 65, no. 2, pp. 832–841, Feb. 2018.

[11] X. Li *et al.*, "Observer-based DC voltage droop and current feed-forward control of a DC microgrid," *IEEE Trans. Smart Grid*, vol. 9, no. 5, pp. 5207–5216, Sep. 2018.

[12] R. Ling, D. Maksimovic, and R. Leyva, "Second-order sliding-mode controlled synchronous buck DC–DC converter," *IEEE Trans. Power Electron.*, vol. 31, no. 3, pp. 2539–2549, Mar. 2016.

[13] C. Zhang, J. Wang, S. Li, B. Wu, and C. Qian, "Robust control for PWM-based DC–DC buck power converters with uncertainty via sampled-data output feedback," *IEEE Trans. Power Electron.*, vol. 30, no. 1, pp. 504–515, Jan. 2015.

[14] J. Wang, S. Li, J. Yang, B. Wu, and Q. Li, "Extended state observer-based sliding mode control for PWM-based DC–DC buck power converter systems with mismatched disturbances," *IET Control Theory Appl.*, vol. 9, no. 4, pp. 579–586, Feb. 2015.

[15] J. Wang, S. Li, J. Yang, B. Wu, and Q. Li, "Finite-time disturbance observer based non-singular terminal sliding-mode control for pulse width modulation based DC–DC buck converters with mismatched load disturbances," *IET Power Electron.*, vol. 9, no. 9, pp. 1995–2002, Jul. 2016.

[16] P.-J. Liu and L.-H. Chien, "A high-efficiency integrated multimode battery charger with an adaptive supply voltage control scheme," *IEEE Trans. Power Electron.*, vol. 33, no. 8, pp. 6869–6876, Aug. 2018.

[17] S. Kapat, P. S. Shenoy, and P. T. Krein, "Near-null response to large-signal transients in an augmented buck converter: A geometric approach," *IEEE Trans. Power Electron.*, vol. 27, no. 7, pp. 3319–3329, Jul. 2012.

[18] J. Lu, S. Golestan, M. Savaghebi, J. C. Vasquez, J. M. Guerrero, and A. Marzabal, "An enhanced state observer for DC-link voltage control of three-phase AC/DC converters," *IEEE Trans. Power Electron.*, vol. 33, no. 2, pp. 936–942, Feb. 2018.

[19] M. Score, "Ceramic or electrolytic output capacitors in DC/DC converters," *Analog Appl. J.*, 2015.

JINGHANG LU (S'14) received the B.Sc. and M.Sc. degrees in electrical engineering from the Harbin Institute of Technology, China, in 2009 and 2011, respectively, the M.Sc. degree in electrical engineering from the University of Alberta, Canada, in 2014, and the Ph.D. degree in power electronics from Aalborg University, Aalborg, Denmark, in 2018.

He is currently with Aalborg University. His research interests include uninterruptible power supply and microgrids.

MEHDI SAVAGHEBI (S'06–M'15–SM'15) was born in Karaj, Iran, in 1983. He received the B.Sc. degree from the University of Tehran, Iran, in 2004, and the M.Sc. and Ph.D. degrees (Hons.) from the Iran University of Science and Technology, Tehran, Iran, in 2006 and 2012, respectively, all in electrical engineering. From 2007 to 2014, he was a Lecturer with the Electrical Engineering Department, Karaj Branch, Islamic Azad University. In 2010, he was a Visiting Ph.D. Student with the Department of Energy Technology, Aalborg University, Aalborg, Denmark, and with the Department of Automatic Control Systems and Computer Engineering, Technical University of Catalonia, Barcelona, Spain.

From 2014 to 2017, he was a Post-Doctoral Fellow with the Department of Energy Technology, Aalborg University, where he was an Associate Professor from 2017 to 2018. He is currently an Associate Professor with the SDU Electrical Engineering Section, Mads Clausen Institute, University of Southern Denmark, Odense, Denmark.

His main research interests include distributed generation systems, microgrids, power quality, and protection of electrical systems, UPS, and smart metering. He is a member of the IEEE Task Force on Microgrid Stability Analysis and Modeling, the IEEE Power and Energy Society, the Technical Committee of Renewable Energy Systems, and the IEEE Industrial Electronics Society. He is the Vice-Chair of the Sub-Committee on Smart Buildings and the IEEE Power and Energy Society. He was a Guest Editor of the Special Issue on Power Quality in Smart Grids and the IEEE TRANSACTIONS ON SMART GRID.

YAJUAN GUAN (S'14–M'16) received the B.S. and M.S. degrees in electrical engineering from Yanshan University, Qinhuangdao, China, in 2007 and 2010, respectively, and the Ph.D. degree in power electronics from Aalborg University, Aalborg, Denmark, in 2016. From 2010 to 2012, she was an Assistant Professor with the Institute of Electrical Engineering, Chinese Academy of Sciences. In 2013, she was a Lecturer with the IEE, CAS. She is currently a Post-Doctoral Fellow with Aalborg University, as part of the Denmark Microgrids Research Programme.

Her research interests include microgrids, distributed generation systems, power converters for renewable energy generation systems, and energy Internet.

JUAN C. VASQUEZ (M'12–SM'14) received the B.S. degree in electronics engineering from the Autonomous University of Manizales, Manizales, Colombia, in 2004, and the Ph.D. degree in automatic control, robotics, and computer vision from the Technical University of Catalonia, Barcelona, Spain, in 2009. He was with the Autonomous University of Manizales as a Teaching Assistant and the Technical University of Catalonia as a Post-Doctoral Assistant in 2005 and 2008, respectively. In 2011, he was an Assistant Professor with the Department of Energy Technology, Aalborg University, Denmark, where he has been an Associate Professor since 2014 and is also the Vice Programme Leader of the Microgrids Research Program. He was a Visiting Scholar with the Center of Power Electronics Systems, Virginia Tech, and a Visiting Professor with Ritsumeikan University, Japan. His current research interests include operation, advanced hierarchical and cooperative control, optimization, and energy management applied to distributed generation in ac/dc microgrids, maritime microgrids, advanced metering infrastructures, and the integration of Internet of Things into the SmartGrid. He is an Associate Editor of the IET Power Electronics and a Guest Editor of the IEEE TRANSACTIONS ON INDUSTRIAL INFORMATICS Special Issue on Energy Internet.

He is currently a member of the IEC System Evaluation Group SEG4 on LVDC Distribution and Safety for the use in Developed and Developing Economies and the Renewable Energy Systems Technical Committee TC-RES in the IEEE Industrial Electronics, PELS, IAS, and PES Societies. In 2017 and 2018, he was a recipient of the Highly Cited Researcher by Thomson Reuters.

AMER M. Y. M. GHIAS (S'10–M'14) received the B.Sc. degree in electrical engineering from Saint Cloud State University, St Cloud, MN, USA, in 2001, the M.Eng. degree in telecommunications from the University of Limerick, Ireland, in 2006, and the Ph.D. degree in electrical engineering from the University of New South Wales (UNSW), Australia, in 2014. From 2002 to 2009, he had held various positions, such as an Electrical Engineer, a Project Engineer, and a Project Manager, with the top companies in Kuwait. He was with UNSW from 2014 to 2015, and with the University of Sharjah, United Arab Emirates, from 2015 to 2018. He is currently an Assistant Professor with the School of Electrical and Electronics Engineering, Nanyang Technological University, Singapore. His research interests include model predictive control of power electronics converters, hybrid energy storage, fault-tolerant converters, modulations, and voltage balancing techniques for multilevel converters, flexible ac transmissions, and high-voltage dc current.

JOSEP M. GUERRERO (S'01–M'04–SM'08–F'15) received the B.S. degree in telecommunications engineering, the M.S. degree in electronics engineering, and the Ph.D. degree in power electronics from the Technical University of Catalonia, Barcelona, in 1997, 2000, and 2003, respectively. Since 2011, he has been a Full Professor with the Department of Energy Technology, Aalborg University, Denmark, where he is responsible for the Microgrid Research Program. Since 2012, he has been a Guest Professor with the Chinese Academy of Sciences and the Nanjing University of Aeronautics and Astronautics; since 2014, he has been the Chair Professor with Shandong University; since 2015, he has been a Distinguished Guest Professor with Hunan University; and since 2016, he has been a Visiting Professor Fellow with Aston University, U.K., and also a Guest Professor with the Nanjing University of Posts and Telecommunications.

His research interests are oriented to different microgrid aspects, including power electronics, distributed energy-storage systems, hierarchical and cooperative control, energy management systems, smart metering and the Internet of Things for ac/dc microgrid clusters, islanded minigrids, and maritime microgrids for electrical ships, vessels, ferries, and seaports. He was a recipient of the Best Paper Award of the IEEE TRANSACTIONS ON ENERGY CONVERSION for the period 2014–2015, the Best Paper Prize of the IEEE-PES in 2015, the Best Paper Award of the *Journal of Power Electronics* in 2016, and the Highly Cited Researcher by Thomson Reuters in 2014, 2015, and 2016. He was the Chair of the Renewable Energy Systems Technical Committee of the IEEE Industrial Electronics Society. He is currently an Associate Editor of the IEEE TRANSACTIONS ON POWER ELECTRONICS, the IEEE TRANSACTIONS ON INDUSTRIAL ELECTRONICS, and the *IEEE Industrial Electronics Magazine*, and an Editor of the IEEE TRANSACTIONS ON SMART GRID and the IEEE TRANSACTIONS ON ENERGY CONVERSION. He has been a Guest Editor of the IEEE TRANSACTIONS ON POWER ELECTRONICS Special Issues: Power Electronics for Wind Energy Conversion and Power Electronics for Microgrids; the IEEE TRANSACTIONS ON INDUSTRIAL ELECTRONICS Special Sections: Uninterruptible Power Supplies systems, Renewable Energy Systems, Distributed Generation and Microgrids, and Industrial Applications and Implementation Issues of the Kalman Filter; the IEEE TRANSACTIONS ON SMART GRID Special Issues: Smart DC Distribution Systems and Power Quality in Smart Grids; and the IEEE TRANSACTIONS ON ENERGY CONVERSION Special Issue on Energy Conversion in Next-generation Electric Ships.

● ● ●